Magnetoelectric effects in multiferroic Y-type hexaferrites Ba$_{0.3}$Sr$_{1.7}$Co$_x$Mg$_{2-x}$Fe$_{12}$O$_{22}$[*]

Yanfen Chang(畅艳芬)[1,2], Kun Zhai(翟昆)[1,2], and Young Sun(孙阳)[1,2,†]

[1] Beijing National Laboratory for Condensed Matter Physics, Institute of Physics, Chinese Academy of Sciences, Beijing 100190, China
[2] School of Physical Science, University of Chinese Academy of Sciences, Beijing 100190, China

Y-type hexaferrites with tunable conical magnetic structures are promising single-phase multiferroics that exhibit large magnetoelectric effects. We have investigated the influence of Co substitution on the magnetoelectric properties in the Y-type hexaferrites Ba$_{0.3}$Sr$_{1.7}$Co$_x$Mg$_{2-x}$Fe$_{12}$O$_{22}$ ($x = 0.0$, 0.4, 1.0, 1.6). The spin-induced electric polarization can be reversed by applying a low magnetic field for all the samples. The magnetoelectric phase diagrams of Ba$_{0.3}$Sr$_{1.7}$Co$_x$Mg$_{2-x}$Fe$_{12}$O$_{22}$ are obtained based on the measurements of magnetic field dependence of dielectric constant at selected temperatures. It is found that the substitution of Co ions can preserve the ferroelectric phase up to a higher temperature, and thus is beneficial for achieving single-phase multiferroics at room temperature.

1. Introduction

The magnetoelectric (ME) multiferroic materials in which magnetism and ferroelectricity coexist have drawn a lot of attention for more than a decade.[1–6] The coexistence of magnetic and ferroelectric orders could enable mutual control of magnetization by an electric field and electric polarization by a magnetic field. Therefore, the ME multiferroics have a great potential for developing new functional devices.[7–9] Although a large number of ME multiferroics have been discovered and investigated,[10–14] single-phase multiferroics with large ME effects are still very limited. Y-type hexaferrites are considered to be one of the most promising single-phase multiferroics due to the intrinsically coupled magnetic and ferroelectric orders at low fields.[15–18] For instance, Zhai et al. obtained the giant ME effects in the Y-type hexaferrite Ba$_{0.4}$Sr$_{1.6}$Mg$_2$Fe$_{12}$O$_{22}$ at 10 K.[19] Hirose et al. reported clear ME effects at room temperature in the Y-type hexaferrite BaSrCo$_2$Fe$_{11}$AlO$_{22}$.[20]

The Y-type hexaferrites with space group $R\bar{3}m$ have a general chemical formula of Ba$_x$Sr$_{2-x}$Me$_2$Fe$_{12}$O$_{22}$ ($Me =$ Mg^{2+}, Co^{2+}, Zn^{2+}, etc.),[21] whose magnetic structure consists of alternating stacks of large (L) and small (S) spin blocks along the c axis,[22] as shown in Fig. 1(a). Previous studies suggest that there are several factors that influence the ME properties of Y-type hexaferrites, such as the annealing process, the sintering temperature, and the ion substitution.[23–25] Extensive studies have been performed to investigate the effects of different ion substitutions on the ME properties of Y-type hexaferrites.[26–29] It was re-

ported that the critical magnetic field for inducing electrical polarization becomes rare low when Mg replaces Zn to form the Y-type hexaferrite Ba$_2$Mg$_2$Fe$_{12}$O$_{22}$.[30,31] Chun et al. showed that the low field ME properties of the Y-type hexaferrites Ba$_{0.5}$Sr$_{1.5}$Zn$_2$(Fe$_{1-x}$Al$_x$)$_{12}$O$_{22}$ can be efficiently tuned by the Al-substitution level.[32] Zhai et al. reported that Sr doping changes the magnetic transition temperature and enhances the ME effects.[19] Hirose et al. found that increasing Co content favors high electrical resistivity.[20,23] In this work, we have prepared a series of Y-type hexaferrites Ba$_{0.3}$Sr$_{1.7}$Co$_x$Mg$_{2-x}$Fe$_{12}$O$_{22}$ ($x = 0.0$, 0.4, 1.0, 1.6) polycrystalline samples, and studied the ME properties in details.

2. Experiment details

Y-type hexaferrites Ba$_{0.3}$Sr$_{1.7}$Co$_x$Mg$_{2-x}$Fe$_{12}$O$_{22}$ ($x =$ 0.0, 0.4, 1.0, 1.6) polycrystalline samples were prepared by the solid-state reaction from starting materials BaCO$_3$, SrCO$_3$, Co$_3$O$_4$, MgO, and Fe$_2$O$_3$. Stoichiometric amounts of powders were thoroughly mixed and ground in an agate mortar. The mixture was calcinated at 1000 °C in air for 14 h. After that, the calcinated mixture was reground, pressed into pellets, sintered at 1200 °C in air for 12 h, annealed at 900 °C in a flow of oxygen atmosphere for 96 h, and cooled down slowly to room temperature at a rate of 50 °C/h. The powder x-ray diffraction (XRD) measurement was carried out at room temperature by using a Rigaku x-ray diffractometer.

The samples were prepared into small plates ($\sim$ 3 mm$\times$4 mm$\times$0.3 mm) and the silver electrodes were painted onto the wildest faces for the measurements of dielec-

[†]Corresponding author. E-mail: youngsun@iphy.ac.cn

http://iopscience.iop.org/cpb   http://cpb.iphy.ac.cn

tric response and ME currents. The dielectric constant was measured by using an LCR meter (Aglient 4980 A) at the frequency of 10 kHz. The ME currents were measured by using an electrometer (Keithley 6517B). They were both carried out in a cryogen-free superconducting magnet system (Oxford Instruments, Teslatron PT). Before measuring the ME currents, the samples were poled in an electric field $E = 500$ kV/m from a high magnetic field of -50 kOe (perpendicular to the electric field) to -5 kOe at a fixed temperature. Then the electric field E was removed and the samples were short-circuited for about 2 h. Finally, the ME currents were measured with time as the magnetic field scanned from -5 kOe to 50 kOe with a sweeping rate 20 Oe/s.

3. Results and discussion

Figure 1(a) illustrates the crystalline structure of the Y-type hexaferrites with a general formula $(Ba, Sr)_2 Me_2 Fe_{12} O_{22}$ ($Me =$ Co, Mg, Ni, etc.) whose space group is $R\bar{3}m$.[21] Alternating small (S) and large (L) magnetic blocks stacking along the [001] direction form the magnetic structure. The magnetic moments are arranged collinearly in each S and L block. Due to the competing exchange interactions, large moments μ_L and small moments μ_S arrange a noncolinear magnetic structure between the blocks. Mg and Co ions partially substitute Fe ions and have a distinct preference for the octahedral sites.[28] Since Co ions carry a magnetic moment, the different ratio of Mg and Co ions will affect the magnetic structure and the ME properties. Figure 1(b) shows the powder XRD patterns of the studied samples at room temperature. A calculated powder XRD pattern of the Y-type hexaferrite structure is also shown in Fig. 1(b) for comparison. The main diffraction peaks can be assigned to the Y-type hexagonal phase.
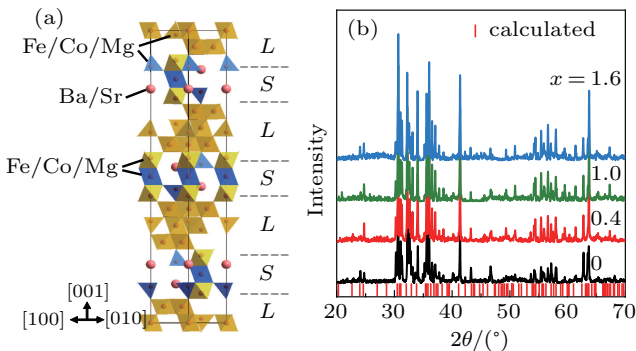

Fig. 1. (a) Schematic crystal structure of Y-type hexaferrites. The magnetic structure consists of alternating stacks of L spin blocks (yellow) and S spin blocks (blue) along [001] direction. (b) The powder XRD patterns of $Ba_{0.3}Sr_{1.7}Co_xMg_{2-x}Fe_{12}O_{22}$ samples at room temperature.

Figures 2(a)–2(d) show the relative change of dielectric constant $\Delta\varepsilon(h)/\varepsilon(50 \text{ kOe}) = [\varepsilon(h) - \varepsilon(50 \text{ kOe})]/\varepsilon(50 \text{ kOe})$ with in-plane magnetic field from -50 kOe to 50 kOe at selected temperatures from 8 K to 300 K for each sample. There are broad peaks at high magnetic fields for all samples,

which are often observed in other Y-type hexaferrites.[33,34] The broad peak indicates the transition from the paraelectric (PE) phase to the ferroelectric (FE) phase. Blow 100 K, there is only a single peak around zero magnetic field for all samples. The magnetodielectric effects of the $x = 0.0$ sample at low temperatures are much larger than those of the other samples. The single peak around zero magnetic field disappears and the double peaks appear when the temperature increases for $x = 0.0$, 0.4, and 1.0. In addition, with further increasing the Co content (x), the temperature at which the single peak appears increases. For $x = 1.6$, there is a single peak at 300 K, which implies the reversal of ferroelectric polarization at room temperature. The typical M–H curves of these samples are shown in Fig. S1 of the supplementary material. The magnetic transitions with increasing magnetic field are not obvious due to the polycrystalline nature of the samples.

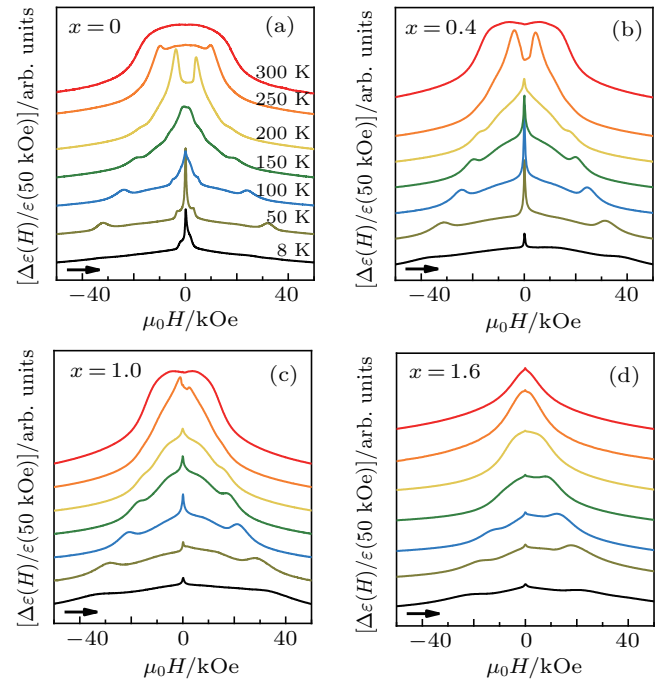**Fig. 2.** (a)–(d) Magnetic field dependence of the relative change of dielectric constant $\Delta\varepsilon(h)/\varepsilon(50 \text{ kOe}) = [\varepsilon(h) - \varepsilon(50 \text{ kOe})]/\varepsilon(50 \text{ kOe})$ for each sample. The arrows indicate the direction of swept magnetic field.

Then we measured the ME current (I) as a function of the magnetic field and obtained the electric polarization by integrating I with time to confirm the spin-induced ferroelectricity, as shown in Figs. 3(a)–3(d). The ME currents are detectable only at low temperatures when the resistivity of the samples is high enough to make an effective electric field poling process. For $x = 0.0$, the electric polarization is measurable up to 50 K. With increasing Co content, the samples become more insulating and the electric polarization can be measured up to 150 K. The maximum electrical polarization reaches about 7.5 μC/m^2 at 50 K for $x = 0.0$, 14 μC/m^2 at 100 K for $x = 0.4$, 7 μC/m^2 at 150 K for $x = 1.0$, and 7.5 μC/m^2 at 100 K for $x = 1.6$. These values of electrical polarizations are smaller than those

reported in single crystals of Y-type hexaferrites.[19] For each sample, the electric polarization reverses its sign when the magnetic field is swept from negative to positive. The reversibility of the spin-induced electric polarization in multiferroic hexaferrites has been discussed in terms of the rotation path of spin cones.[35] The reversal of electric polarization upon the reversal of magnetization suggests that the spin cones rotate in the *ab* plane in these samples.
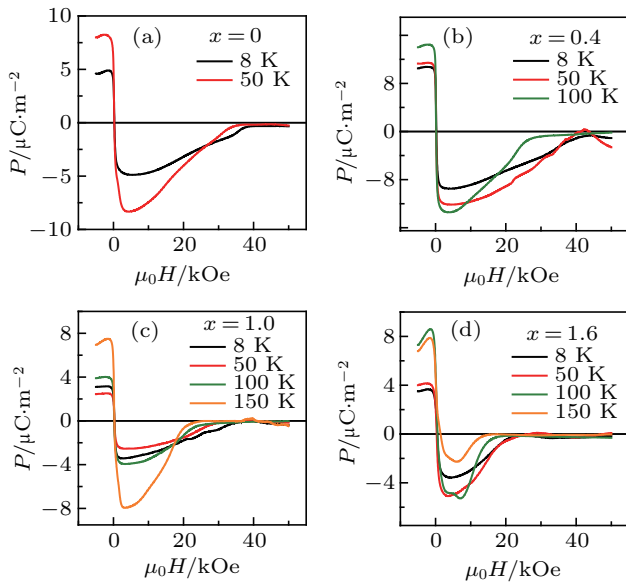

Fig. 3. (a)–(d) Magnetic field reversal of electric polarization at selected temperatures for $x = 0.0$, 0.4, 1.0, and 1.6, respectively.
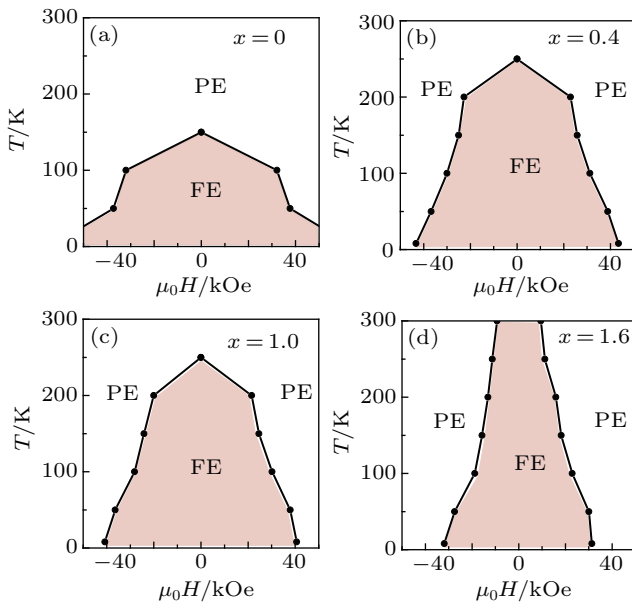

Fig. 4. (a)–(d) Magnetoelectric phase diagram of $Ba_{0.3}Sr_{1.7}Co_xMg_{2-x}Fe_{12}O_{22}$ with $x = 0.0$, 0.4, 1.0, and 1.6, respectively. The phase boundaries are determined from the critical fields where the dielectric constant shows a peak with increasing magnetic field.

The ME phase diagrams of all the samples are shown in Figs. 4(a)–4(d), which are based on the magnetic field dependence of the dielectric constant at selected temperatures. The critical magnetic fields at which the dielectric constant shows

peaks determine the phase boundaries between paraelectric (PE) and ferroelectric (FE). The PE phase with the collinear magnetic structure is in the high magnetic field region. The FE phase shows up in the low magnetic field region where conical magnetic structures exist. With increasing Co content, the FE phase extends to higher temperatures and the critical magnetic field is lowered. For $x = 1.6$, the FE phase is expected to be preserved up to room temperature. The M–T curve of $Ba_{0.3}Sr_{1.7}Co_xMg_{2-x}Fe_{12}O_{22}$ ($x = 1.6$) is shown in Fig. S2 of the supplementary material. The sample has a paramagnetic to collinear ferrimagnetic transition at $T_C \sim 760$ K. The shoulder in the M–T curve around T_1 (~ 410 K) represents the magnetic transition into a spiral magnetic ordering.[23] Since T_1 is above room temperature, it indicates that the ME coupling can be obtained at room temperature.

4. Conclusions

In summary, we have investigated the ME effects in multiferroic Y-type hexaferrites $Ba_{0.3}Sr_{1.7}Co_xMg_{2-x}Fe_{12}O_{22}$ ($x = 0.0$, 0.4, 1.0, 1.6) and obtained their ME phase diagrams. The electric polarization can be reversed by a small magnetic field for all the samples at selected temperatures. With increasing Co content, the resistivity of the samples increases so that the spin-induced ferroelectricity is measurable at a higher temperature. Meanwhile, the magnetic interaction between Co and Fe ions may further stabilize the spiral magnetic structure. As a result, the FE phase extends to higher temperatures with increasing Co level. These results suggest that Co substitution favors room-temperature multiferroicity in hexaferrites.

References

[1] Hur N, Park S, Sharma P A, Ahn J S, Guha S and Cheong S W 2004 *Nature* **429** 392
[2] Spaldin N A and Fiebig M 2005 *Science* **309** 391
[3] Eerenstein W, Mathur N D and Scott J F 2006 *Nature* **442** 759
[4] Ramesh R and Spaldin N A 2007 *Nat. Mater.* **6** 21
[5] Scott J F 2007 *Nat. Mater.* **6** 256
[6] Fiebig M 2005 *J. Phys. D* **38** R123
[7] Kimura T, Goto T, Shintani H, Ishizaka K, Arima T and Tokura Y 2003 *Nature* **426** 55
[8] Chu Y H, Martin L W, Holcomb M B, Gajek M, Han S J, He Q, Balke N, Yang C H, Lee D, Hu W, Zhan Q, Yang P L, Rodríguez A F, Scholl A, Wang S X and Ramesh R 2008 *Nat. Mater.* **7** 478
[9] Ebnabbasi K, Mohebbi M, Vittoria C 2013 *J. Appl. Phys.* **113** 17C703
[10] Kitagawa Y, Hiraoka Y, Honda T, Ishikura T, Nakamura H and Kimura T 2010 *Nat. Mater.* **9** 797
[11] Mohebbi M, Ebnabbasi K, Vittoria C 2013 *J. Appl. Phys.* **113** 17C710
[12] Zheng H, Wang J, Lofland S E, Ma Z, Mohaddes-Ardabili L, Zhao T, Salamanca-Riba L, Shinde S R, S Ogale S B, Bai F, Viehland D, Jia Y, Schlom D G, Wuttig M, Roytburd A and Ramesh R 2004 *Science* **303** 661
[13] Okumura K, Ishikura T, Soda M, Asaka T, Nakamura H, Wakabayashi Y and Kimura T 2011 *Appl. Phys. Lett.* **98** 212504
[14] Tokunaga Y, Kaneko Y, Okuyama D, Ishiwata S, Arima T, Wakimoto S, Kakurai K, Taguchi Y and Tokura Y 2010 *Phys. Rev. Lett.* **105** 257201
[15] Kimura T, Lawes G, Ramirez A P 2005 *Phys. Rev. Lett.* **94** 137201
[16] Wang F, Zou T, Yan L, Yi L and Sun Y 2012 *Appl. Phys. Lett.* **100** 122901

[17] Kimura T 2012 *Annu. Rev. Condens. Matter Phys.* **3** 93

[18] Wang G, Cao S, Cao Y, Hu S, Wang X, Feng Z, Kang B, Chai Y, Zhang J and Ren W 2015 *J. Appl. Phys.* **118** 094102

[19] Zhai K, Wu Y, Shen S, Tian W, Cao H, Chai Y, Chakoumakos B C, Shang D, Yan L, Wang F and Sun Y 2017 *Nat. Commun.* **8** 519

[20] Hirose S, Haruki K, Ando A and Kimura T 2014 *Appl. Phys. Lett.* **104** 022907

[21] Kohn J A, Eckart D W and Cook C F 1971 *Science* **172** 519

[22] Momozawa N, Yamaguchi Y, Takei H and Mita M 1985 *J. Phys. Soc. Jpn.* **54** 771

[23] Hirose S, Haruki K, Ando A and Kimura T 2015 *J. Am. Ceram. Soc.* **98** 2104

[24] Pullar R C 2012 *Prog. Mater. Sci.* **57** 1191

[25] Kwon S, Kang B, Kim C, Jo E, Lee S, Chai Y S, Chun S H and Kim K H 2014 *J. Phys.: Condens. Matter* **26** 146004

[26] Utsumi S, Yoshiba D and Momozawa N 2007 *J. Phys. Soc. Jpn.* **76** 034704

[27] Won M H and Kim C S 2013 *J. Appl. Phys.* **113** 17D906

[28] Albanese G, Carbucicchio M, Deriu A, Asti G and Rinaldi S 1975 *Appl. Phys.* **7** 227

[29] Chang H, Lee H B, Song Y S, Chung J H, Kim S A, Oh I H, Reehuis M and Schefer J 2012 *Phys. Rev. B* **86** 059905

[30] Ishiwata S, Taguchi Y, Murakawa H, Onose Y and Tokura Y 2008 *Science* **319** 1643

[31] Taniguchi K, Abe N, Ohtani S, Umetsu H and Arima T H 2008 *Appl. Phys. Express* **1** 031301

[32] Chun S H, Chai Y S, Oh Y S, Jaiswal-Nagar D, Haam S Y, Kim I, Lee B, Nam D H, Ko K T, Park J H, Chung J and Kim K H 2010 *Phys. Rev. Lett.* **104** 037204

[33] Chang Y, Zhai K, Chai Y, Shang D and Sun Y 2018 *J. Phys. D: Appl. Phys.* **51** 264002

[34] Shen S, Yan L, Chai Y, Cong J and Sun Y 2014 *Appl. Phys. Lett.* **104** 032905

[35] Shen S, Liu X, Chai Y, Studer A J, He C, Wang S and Sun Y 2019 *Phys. Rev. B* **100** 134433